ChemComm

www.rsc.org/chemcomm

COMMUNICATION

One pot glucose detection by [Fe^{III}(biuret-amide)] immobilized on mesoporous silica nanoparticles: an efficient HRP mimic†

Bharmana Malvi, Chakadola Panda, Basab B. Dhar and Sayam Sen Gupta*

An [Fe^{III}(biuret-amide)] complex has been immobilized onto mesoporous silica nanoparticles *via* Cu(ɪ) catalyzed azide–alkyne click chemistry. This hybrid material functions as an efficient peroxidase mimic and was successfully used for the quantitative determination of hydrogen peroxide and glucose *via* a one-pot colorimetric assay.

Peroxidases are ubiquitous in nature and are known to activate hydrogen peroxide to perform a variety of chemical reactions such as oxidations.[1] They have been extensively studied for many industrial applications such as bleaching inducers, for example, in the detergent and pulp industries.[2] Although, peroxidases have potential commercial applications in many different areas, the most developed field for their commercial application is analytical diagnostics.[1,3] For example, horseradish peroxidase (HRP), a heme-containing peroxidase, is widely used for detection of glucose and in immunoassays where the key step is the peroxidase catalyzed conversion of a non-luminescent substrate into a luminescent one, thus amplifying the signal many fold.[4] However, limited stability of these enzymes (gets denatured upon heating or chemical changes) and the relatively low productivities (preparation, purification and storage are time consuming) are important features which hinder the commercial application of HRP. Hence, for several decades a significant amount of research has been carried out to make systems that mimic HRP. Small molecule analogs that have been reported include synthetic porphyrins, sulfonated phthalocyanines and Fe-TAML's.[5] Recently, various nano-materials including Fe$_3$O$_4$ magnetic NPs,[6] positively charged gold NPs,[7] cupric oxide NPs,[8a] ceria NPs,[8b] graphene oxide,[8c] CNTs,[8d] carbon nanodots[8e] and folate-polyoxometalate hybrid spheres[8f] have been reported to possess peroxidase like activity and have been used for the visual detection of H$_2$O$_2$ and glucose. But these NPs display peroxidase activity only in acidic pH, which makes their application as biosensor unwieldy. For example, quantitative detection of glucose by these NPs involves a
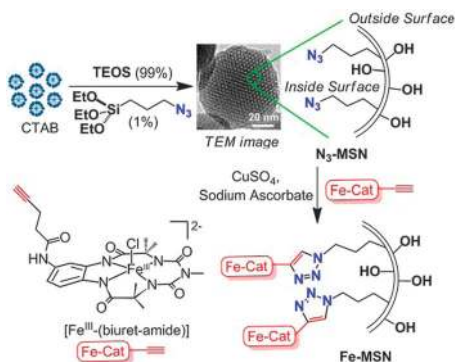
two step process: first incubation of glucose with glucose oxidase (GOX) at pH 7.4 to generate H$_2$O$_2$ and then subsequent incubation of this glucose reaction mixture with NPs at low pH ($\sim$4) to oxidize a peroxidase substrate like 3,3′,5,5′-tetramethylbenzidine (TMB) to generate a visual signal.[6b,7,8a] Thus there is a need for the development of robust materials that can be used as biosensors[9] and in immunoassays at physiological pH of 7.4.

We hereby report the synthesis of a mesoporous silica nanoparticles (MSNs) based hybrid material (Fe-MSN) that mimics the enzyme HRP and functions as a biosensor at physiological pH. This hybrid material contains a robust small molecule peroxidase mimic [Fe^{III}(biuret-amide)] developed in our group[10] that is covalently attached to azide containing MSN particles by Cu(ɪ) catalyzed azide alkyne cycloaddition reaction (CuAAC).[11] Fe-MSN has several attributes that make it very attractive: (i) the small molecule peroxidase mimic [Fe^{III}(biuret-amide)] in Fe-MSN exhibits excellent reactivity and very high stability, especially at low pH and high ionic strength;[10] (ii) the co-condensation method used to synthesize the azide grafted material allows the attachment of [Fe^{III}(biuret-amide)] catalyst mostly inside the MSN pore which limits its interaction with enzymes like GOX during one-pot glucose detection;[12] (iii) usage of MSN particles having 1% azide groups also allows reasonable site-isolation of the catalyst and this is expected to reduce intermolecular degradation of the catalyst as has been shown before;[11c,13] and (iv) the silanol groups on the outer surface of MSN can be further functionalized to incorporate targeting ligands such as antigens/antibodies for usage in immunoassays like ELISA. The synthesized Fe-MSN nanoparticles were characterized by several techniques such as FT-IR, EPR, ICP and nitrogen adsorption–desorption experiments. We also show that these hybrid MSN particles can be used as a biosensor for the quantitative detection of H$_2$O$_2$ and glucose in a one-pot method.

The azide functionalized mesoporous silica nanoparticles (N$_3$-MSN) were prepared by one pot co-condensation of TEOS and 3-azidopropyl triethoxysilane (AzPTES) in the molar ratio of 99 : 1 (Scheme 1).[14] After template removal, the resultant material was analyzed by a variety of analytical techniques (ESI†). The amount of azide groups grafted on the surface of N$_3$-MSN was determined to be 0.12 mmol g^{-1} by elemental analysis and TGA (Fig. S6, ESI†). XRD, TEM and SEM showed formation of well-ordered two-dimensional hexagonal mesoporous particles with a spherical morphology

CReST Unit, Chemical Engineering Div.,
National Chemical laboratory, Dr. Homi Bhabha Road, Pune,
411008, India. E-mail: ss.sengupta@ncl.res.in;
Fax: +91 20 25902621; Tel: +91 20 25902747
† Electronic supplementary information (ESI) available: Experimental details and characterizations of MSN's and catalysts. See DOI: 10.1039/c2cc30970j
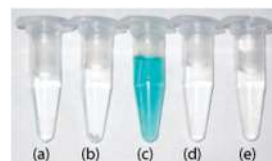
Scheme 1 Synthesis of [Fe^{III}(biuret-amide)] functionalized MSN.

Fig. 1 Typical images of: (a) TMB and H$_2$O$_2$ in the absence of Fe-MSN, (b) TMB and Fe-MSN in the absence of H$_2$O$_2$, (c) TMB and H$_2$O$_2$ in the presence of Fe-MSN, (d) TMB and H$_2$O$_2$ in the presence of N$_3$-MSN and (e) TMB and H$_2$O$_2$ in the presence of propargyl alcohol clicked MSN particles (PrOH-MSN). Experimental conditions: 10 μL of TMB solution, 747 μL of de-ionized water, 133 μL of phosphate buffer (150 mM, pH 7), 200 μL H$_2$O$_2$ solution (10 mM) and 10 μL of catalyst solution.

having particle size of 100 $\pm$ 10 nm (Fig. S2 and S3, ESI†). Nitrogen adsorption–desorption showed the multi-point BET surface area, pore diameter and pore volume to be 724 m^2 g^{-1}, 2.4 nm and 0.93 cc g^{-1} respectively (Fig. S4(a), Table S1, ESI†). These values are consistent with those of the other organo-functionalized mesoporous silica nanoparticles reported earlier.[14] Since the MSN particles had the organoazide group attached to their surface, the metal complex [Fe^{III}(biuret-amide)] having a pendent alkyne group was synthesized so that it can be attached to the N$_3$-MSN using CuAAC. The detailed synthetic scheme and characterization of the [Fe^{III}(biuret-amide)]–alkyne catalyst are described in ESI.†

The azidopropyl labelled MSN nanoparticle, N$_3$-MSN, was then subjected to CuAAC with the [Fe^{III}(biuret-amide)]–alkyne complex using CuSO$_4$ and sodium ascorbate as described in the literature.[11a,c,15] Efficient removal of copper during the washing has been observed by the absence of copper in ICP analysis. The extent of click reaction was estimated by IR spectroscopy[11a] (Fig. S5, ESI†), TGA and ICP analysis and the amount of catalyst incorporated was estimated by ICP to be 0.048 mmol of [Fe^{III}(biuret-amide)] per gram of Fe-MSN. TGA showed incorporation of 0.056 mmol g^{-1} [Fe^{III}(biuret-amide)] complex per gram of Fe-MSN (Fig. S6, ESI†). The EPR spectrum of Fe-MSN displayed a resonance at g = 4.2 and 1.96 which is characteristic of the [Fe^{III}(biuret-amide)] complex (Fig. S7, ESI†). Hence TGA, ICP, EPR and IR spectroscopy data indicate successful incorporation of the [Fe^{III}(biuret-amide)] complex onto the surface of MSN particles *via* CuAAC reaction. The N$_2$ adsorption–desorption isotherm of Fe-MSN displayed a similar profile to its parent N$_3$-MSN, which indicates that the material did not undergo any physical change during the course of the click reaction and its subsequent workup (Fig. S4(b), ESI†).

To investigate the peroxidase like activity of the Fe-MSN particles, the catalytic oxidation of peroxidase substrate 3,3′,5,5′-tetramethylbenzidine (TMB) in the presence of hydrogen peroxide was tested (Fig. 1). Catalytic oxidation of TMB by Fe-MSN in the presence of H$_2$O$_2$ yields a blue colored solution. The blue color of the solution results from the product formed by the oxidation of TMB, which gives a maximum absorbance at 650 nm in the UV-Vis spectrum. To confirm that the blue color is formed because of the catalytic activity of the [Fe^{III}(biuret-amide)] complex anchored on the surface of MSN's, a series of control experiments were carried out using azide functionalized MSN particles (N$_3$-MSN) and propargyl alcohol clicked MSN particles (PrOH-MSN).

Both the materials did not produce blue color in the solution even after 3 h of incubation time. Thus the blue color of the solution originates from the catalytic activity of the [Fe^{III}(biuret-amide)] complex anchored on the MSN particles. Since the catalytic activity of the Fe-MSN is dependent on the concentration of the hydrogen peroxide in the solution, this method can be used for the quantitative estimation of hydrogen peroxide. Fig. 2 shows the change in absorbance at 650 nm with increase in the concentration of the hydrogen peroxide in solution. The calibration graph of the absorbance at 650 nm to concentration of hydrogen peroxide is linear in the range 1.0×10^{-4} to 5.0×10^{-3} M with a detection limit at 1.0×10^{-5} M.

To investigate the peroxidase like activity of Fe-MSN, we studied the apparent steady-state kinetic parameters for the reaction. The kinetic data were fitted perfectly to a typical Michaelis–Menten curve (Fig. S8 and S9, ESI†). The K_m (Michaelis constant) and V_{max} (maximal reaction velocity) values determined from the Michaelis–Menten curve are given in Table 1. The K_m value of the Fe-MSN with H$_2$O$_2$ as the substrate was significantly higher than that of HRP[6a] (Table 1) consistent with the observation that a higher concentration of H$_2$O$_2$ was required to observe maximal activity for the Fe-MSN whereas the K_m value of the Fe-MSN with TMB as the substrate was about 10 times lower than that of HRP, suggesting that the Fe-MSN have a higher affinity for TMB than HRP.[6a]

Further, we extended the peroxidase like activity of the Fe-MSN particles for the detection of glucose by coupling the above catalytic reaction with glucose oxidation reaction by glucose oxidase (GOX). The GOX oxidizes glucose to form
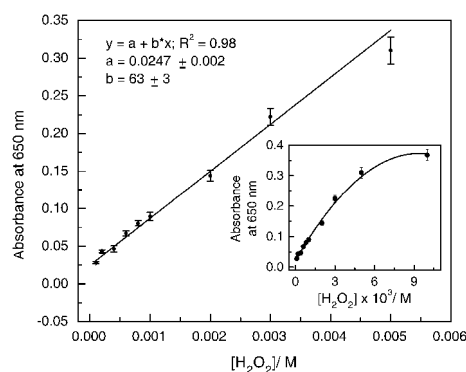
Fig. 2 Linear calibration plot between the absorbance at 650 nm and concentration of H$_2$O$_2$ at pH 7. The inset shows the dependence of the absorbance at 650 nm on the concentration of H$_2$O$_2$ in the range 0.1 mM to 10 mM.

Table 1 Comparison of kinetic parameters of TMB oxidation by Fe-MSN and HRP

Catalyst	Substrate	V_{max}/M s^{-1}	K_m/M
Fe-MSN	TMB	1.01×10^{-8}	1.58×10^{-5}
	H_2O_2	1.41×10^{-6}	5.2×10^{-1}
HRP[6a]	TMB	10.0×10^{-8}	4.34×10^{-4}
	H_2O_2	8.71×10^{-8}	3.70×10^{-3}
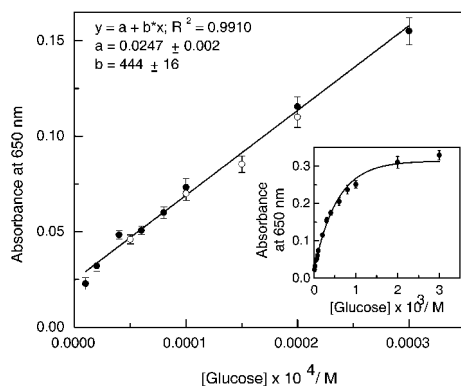
Fig. 3 (●) Linear calibration plot between the absorbance at 650 nm and concentration of glucose at pH 7.4. The inset shows the dependence of the absorbance at 650 nm on the concentration of glucose in the range 0.01 mM to 3 mM. (○) Glucose in mice blood plasma analysis.

gluconic acid and H_2O_2 quantitatively; the H_2O_2 thus produced is then utilized by Fe-MSN to oxidize TMB to produce a blue colored solution. Using this methodology, the calibration graph of the absorbance at 650 nm to concentration of glucose was found to be linear in the range 2.0×10^{-5} to 3.0×10^{-4} M with a detection limit of 1.0×10^{-5} M under the experimental conditions (Fig. 3). The limit of detection (LOD) of Fe-MSN is slightly lower than that of gold nanoparticles[7] (LOD 1.8×10^{-5} M) and Fe_3O_4 nanoparticles[6b] (LOD 5×10^{-5} M). Our methodology also allows detection of glucose in one pot reaction at physiological pH in which the GOX, glucose and Fe-MSN are all added together. This is in contrast to most other literature methods using nanoparticles which use a two-step process as described before. In Fe-MSN nanoparticles, most of the [Fe^{III}(biuret-amide)] catalysts are anchored inside the 2.3 nm pore channels which allows access to small molecules such as H_2O_2 and TMB while large molecules like glucose oxidase are excluded since they cannot enter the pore channels because of their large size. As a result, multistep reactions occur at two different parts of the material, *i.e.* generation of H_2O_2 from glucose using GOX occurs outside the pore channels while the oxidation of TMB by the [Fe^{III}(biuret-amide)] complex takes place inside the pore channels. This allows two different catalytic reactions to proceed simultaneously at two parts of the material without interfering with each other. Further, control experiments using 5 mM of fructose, maltose and lactose showed the specificity of the developed method towards glucose as no detectable color was observed in control reactions (Fig. S10, ESI†). Finally, in order to test that our methodology works in real sample analysis, experiments were carried out with mice blood plasma containing 5.88 mM glucose (ESI†). The average concentration of glucose in mice blood plasma was determined by the above described methodology

to be 5.77 mM (Fig. 3 and ESI†). Thus, this study demonstrates that Fe-MSN can be used for the analysis of real samples.

In conclusion, we have reported immobilization of the [Fe^{III}(biuret-amide)] complex on mesoporous silica nanoparticles using Cu(I) catalyzed azide alkyne click chemistry. This organic–inorganic hybrid material functions as an efficient peroxidase mimic and has been used successfully for the colorimetric assay of H_2O_2 and glucose in one-pot. Further, the presence of silanol groups on the outer surface of Fe-MSN allows easy functionalization to install targeting ligands so that these materials can be used for immunoassays. Such work is ongoing in our laboratory.

Notes and references

1 H. B. Dunford, *Heme Peroxidases*, Wiley-VCH, New York, 1999; M. P. J. van Deurzen, F. van Rantwijk and R. A. Sheldon, *Tetrahedron*, 1997, **53**, 13183.
2 P. Peralta-Zamora, E. Esposito, R. Pelegrini, R. Groto, J. Reyes and N. Durán, *Environ. Technol.*, 1998, **19**, 55.
3 Y. P. Chau and K. S. Lu, *Cells Tissues Organs*, 1995, **153**, 135.
4 T. P. Whitehead, G. H. G. Thorpe, T. J. N. Carter, C. Groucutt and L. J. Kricka, *Nature*, 1983, **305**, 158; V. Sanz, S. de Marcos, J. R. Castillo and J. Galbán, *J. Am. Chem. Soc.*, 2005, **127**, 1038.
5 A. Brausam, S. Eigler, N. Jux and R. van Eldik, *Inorg. Chem.*, 2009, **48**, 7667; M. Nango, T. Iwasaki, Y. Takeuchi, Y. Kurono, J. Tokuda and R. Oura, *Langmuir*, 1998, **14**, 3272; T. J. Collins, *Acc. Chem. Res.*, 2002, **35**, 782; R. A. W. Johnstone, P. A. Stocks and A. J. Simpson, *Chem. Commun.*, 1997, 2277.
6 (a) L. Z. Gao, J. Zhuang, L. Nie, J. B. Zhang, Y. Zhang, N. Gu, T. H. Wang, J. Feng, D. L. Yang, S. Perrett and X. Yan, *Nat. Nanotechnol.*, 2007, **2**, 577; (b) H. Wei and E. Wang, *Anal. Chem.*, 2008, **80**, 2250.
7 Y. Jv, B. X. Li and R. Cao, *Chem. Commun.*, 2010, **46**, 8017.
8 (a) W. Chen, J. Chen, A. L. Liu, L. M. Wang, G. W. Li and X. H. Lin, *ChemCatChem*, 2011, **3**, 1151; (b) M. Ornatska, E. Sharpe, D. Andreescu and S. Andreescu, *Anal. Chem.*, 2011, **83**, 4273; A. Asati, S. Santra, C. Kaittanis, S. Nath and J. M. Perez, *Angew. Chem., Int. Ed.*, 2009, **48**, 2308; (c) Y. Song, K. Qu, C. Zhao, J. Ren and X. Qu, *Adv. Mater.*, 2010, **22**, 2206; (d) Y. Song, X. Wang, C. Zhao, K. Qu, J. Ren and X. Qu, *Chem.–Eur. J.*, 2010, **16**, 3617; (e) W. Shi, Q. Wang, Y. Long, Z. Cheng, S. Chen, H. Zheng and Y. Huang, *Chem. Commun.*, 2011, **47**, 6695; (f) J. Wang, X. Mi, H. Guan, X. Wang and Y. Wu, *Chem. Commun.*, 2011, **47**, 2940.
9 M. Zhou and S. Dong, *Acc. Chem. Res.*, 2011, **44**, 1232; M. Zhou, Y. Zhai and S. Dong, *Anal. Chem.*, 2009, **81**, 5603.
10 C. Panda, M. Ghosh, T. Panda, R. Banerjee and S. Sen Gupta, *Chem. Commun.*, 2011, **47**, 8016.
11 (a) B. Malvi, B. R. Sarkar, D. Pati, R. Mathew, T. G. Ajithkumar and S. Sen Gupta, *J. Mater. Chem.*, 2009, **19**, 1409; (b) A. Schlossbauer, D. Schaffert, J. Kecht, E. Wagner and T. Bein, *J. Am. Chem. Soc.*, 2008, **130**, 12558; (c) J. Nakazawa and T. D. P. Stack, *J. Am. Chem. Soc.*, 2008, **130**, 14360.
12 S. Huh, J. W. Wiench, J.-C. Yoo, M. Pruski and V. S. Y. Lin, *Chem. Mater.*, 2003, **15**, 4247; Y. Huang, S. Xu and V. S. Y. Lin, *Angew. Chem., Int. Ed.*, 2011, **50**, 661.
13 J. Nakazawa, B. J. Smith and T. D. P. Stack, *J. Am. Chem. Soc.*, 2012, **134**, 2750.
14 C.-Y. Lai, B. G. Trewyn, D. M. Jeftinija, K. Jeftinija, S. Xu, S. Jeftinija and V. S. Y. Lin, *J. Am. Chem. Soc.*, 2003, **125**, 4451; R. Mortera, J. Vivero-Escoto, I. I. Slowing, E. Garrone, B. Onida and V. S. Y. Lin, *Chem. Commun.*, 2009, 3219.
15 V. Hong, S. I. Presolski, C. Ma and M. G. Finn, *Angew. Chem., Int. Ed.*, 2009, **48**, 9879.